TABLE OF CONTENTS

Appendix Figures and Figure legends

Appendix Figure S1

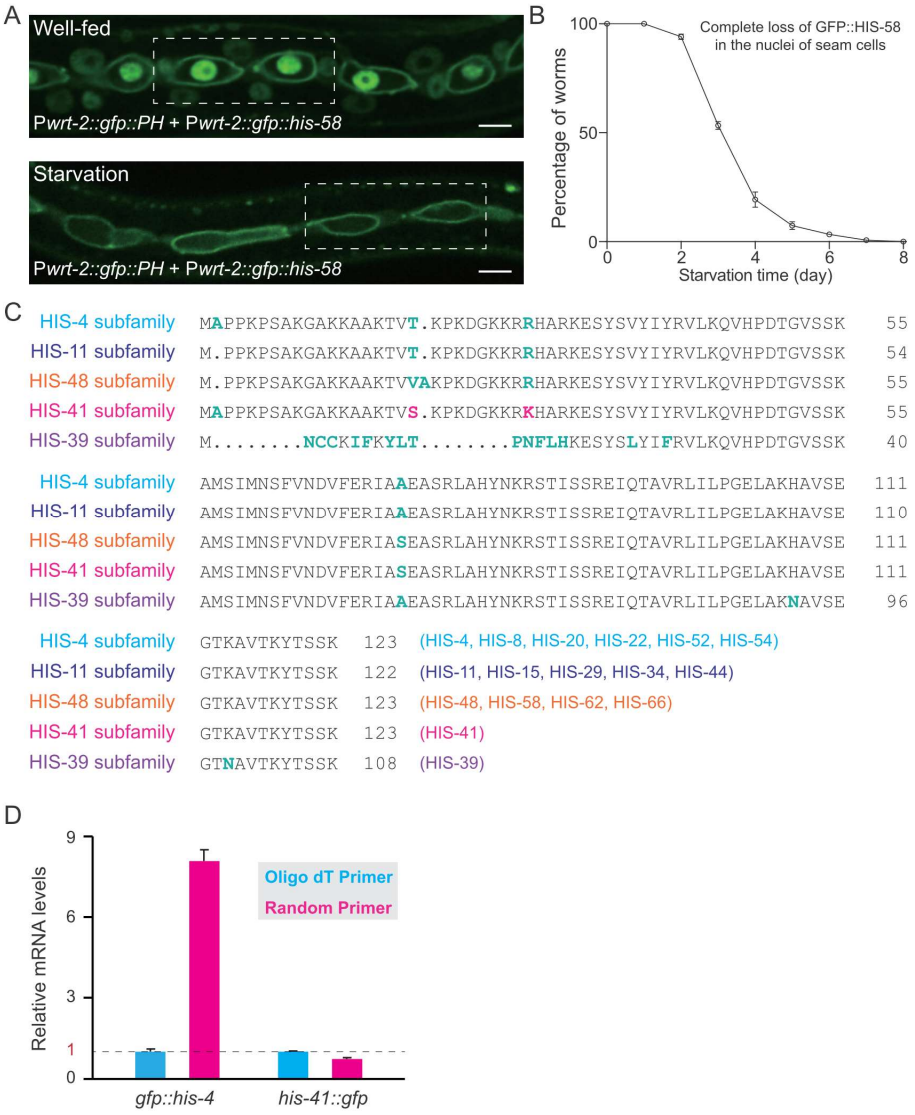

Appendix Figure S1. H2B degradation during starvation in *C. elegans*. (A) Fluorescence images of seam cells in transgenic animals. The GFP::PH (Pleckstrin homology domain) and GFP::HIS-58 (H2B) were expressed under the control of an epidermal seam cell-specific *wrt-2* promoter. Images in the white dotted boxes are shown in Figure 1A. Scale bar, 5 μm. **(B)** Quantification of transgenic animals expressing GFP::HIS-58 fluorescence signals during starvation. Three independent assays (n = 300) were conducted for each time point. Note: We detected fluorescence reduction several hours after starving the animals, but we only scored the loss of

GFP::H2B when we could not detect any GFP::H2B fluorescence from any seam cells in the animal. **(C)** Alignment of the amino-acid sequence of H2B in *C. elegans*. Amino acids with colors indicate sequence variations of *C. elegans* H2B proteins. Magenta residues are unique to HIS-41. **(D)** qRT–PCR showing relative expression levels of the *gfp::his-4* or *his-41::gfp* mRNA in well-fed larval animals using oligo or random primer. Relative RNA levels (normalized to *rps-4*) are normalized to the result of the oligo primer. Three biological replicates and three technical replicates were performed. Data shown are means ± SEM.

Appendix Figure S2

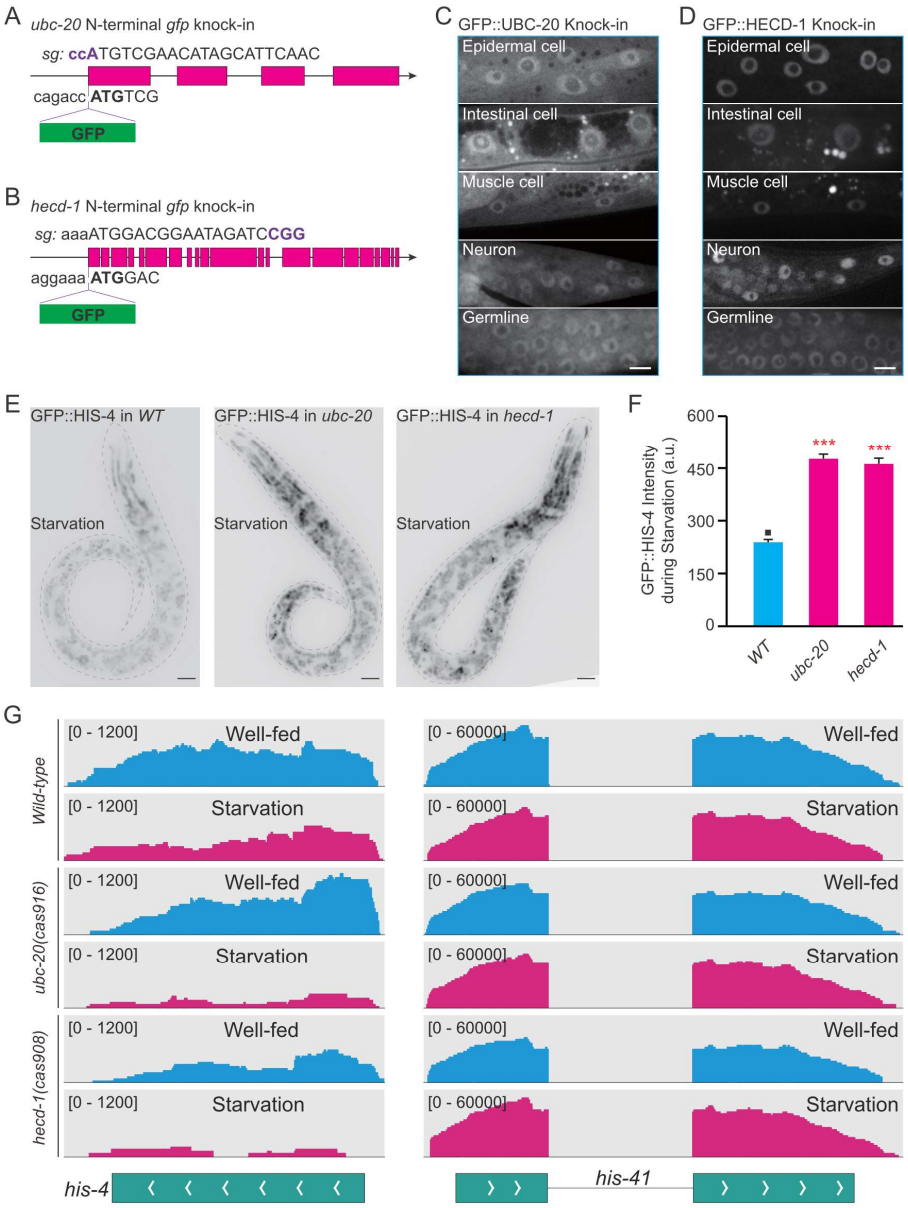

Appendix Figure S2. UBC-20 and HECD-1 regulate endogenous H2B degradation during starvation. (A-B) Schematic illustration of GFP knock-in of *ubc-20* (A) and *hecd-1* (B) by CRISPR-Cas9-based genome editing. The sgRNA sequence and PAM site used to target *ubc-20* or *hecd-1* are shown. **(C-D)** Fluorescence images of GFP-tagged UBC-20 and HECD-1 localization in multiple cell types of *C. elegans*. Scale bar, 5 μm. **(E)** Fluorescence inverted images of GFP::HIS-4 KI in *WT*, *ubc-20(cas916),* and *hecd-1(cas908)* animals during starvation. Images were inverted so that the GFP

fluorescence intensity was black. Dashed lines show the animal periphery. Scale bar, 5 μm. **(F)** Quantification of the endogenous GFP::HIS-4 fluorescence in starved animals with different genotypes (each genotype n = 32). Data shown are means ± SEM; *P* values were determined by a two-tailed unpaired t-test, ***$P < 0.001$. **(G)** Genome browser tracks of RNA-seq peaks with different genotypes at the *his-4* or *his-41* locus in well-fed and starved animals.

Appendix Figure S3

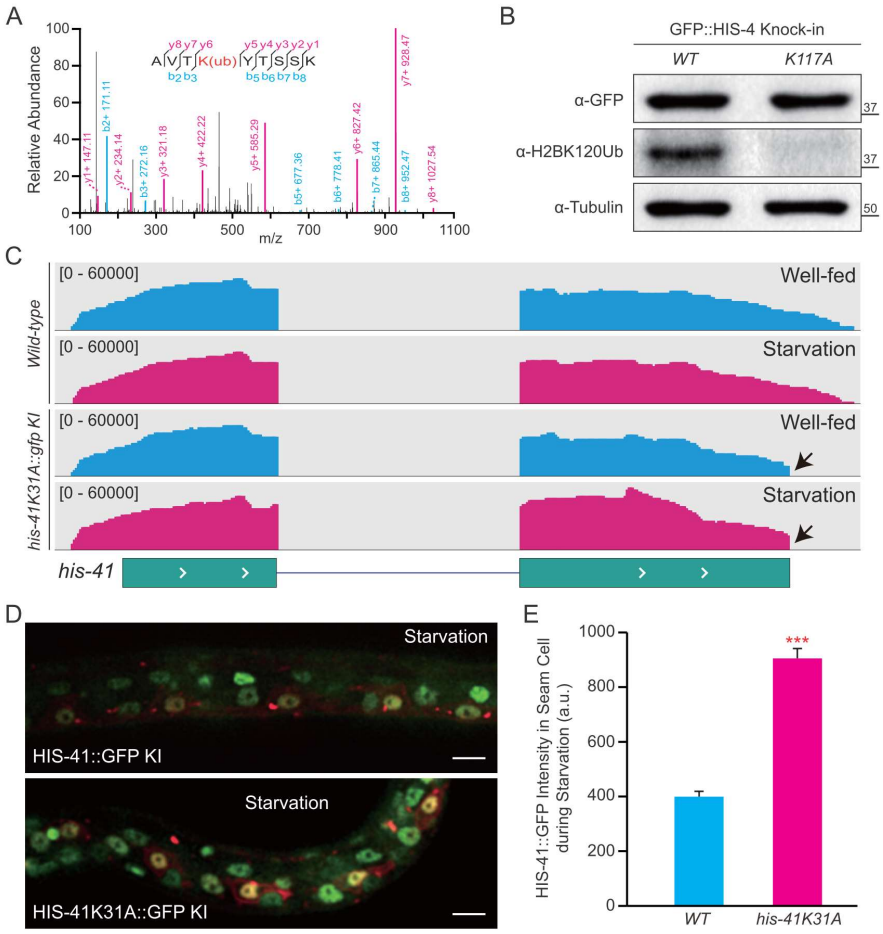

Appendix Figure S3. Histone H2BK31 is required for H2B degradation during starvation. (A) Tandem mass spectrum of the K117ub modified peptide from GFP::HIS-4 KI animals. The y and b series indicate fragments at amide bonds of the peptide. K117 of the *C. elegans* H2B/HIS-4 corresponds to K120 of the human H2B. **(B)** Immunoblot analysis of endogenous GFP::HIS-4 and GFP::HIS-4^{K117A} protein levels in well-fed animals. **(C)** Genome browser tracks of RNA-seq peaks with different genotypes at the *his-41* locus in well-fed and starved animals. The arrows indicate that *his-41* mRNA peaks were interrupted by an inserted *gfp* element. **(D)** Fluorescence images of HIS-41::GFP KI and HIS-41^{K31A}::GFP KI during starvation. The mCherry::PH (membrane) and mCherry::HIS-24 (histone H1, nucleus) were expressed under the control of a seam cell-specific *ceh-16* promoter. Scale bar, 5 μm. **(E)** Quantification of endogenous HIS-41::GFP and HIS-41^{K31A}::GFP fluorescence in the

nucleus of seam cells during starvation (each genotype n = 100). Data shown are means ± SEM; *P* values were determined by a two-tailed unpaired t-test, ***$P < 0.001$.

Appendix Figure S4

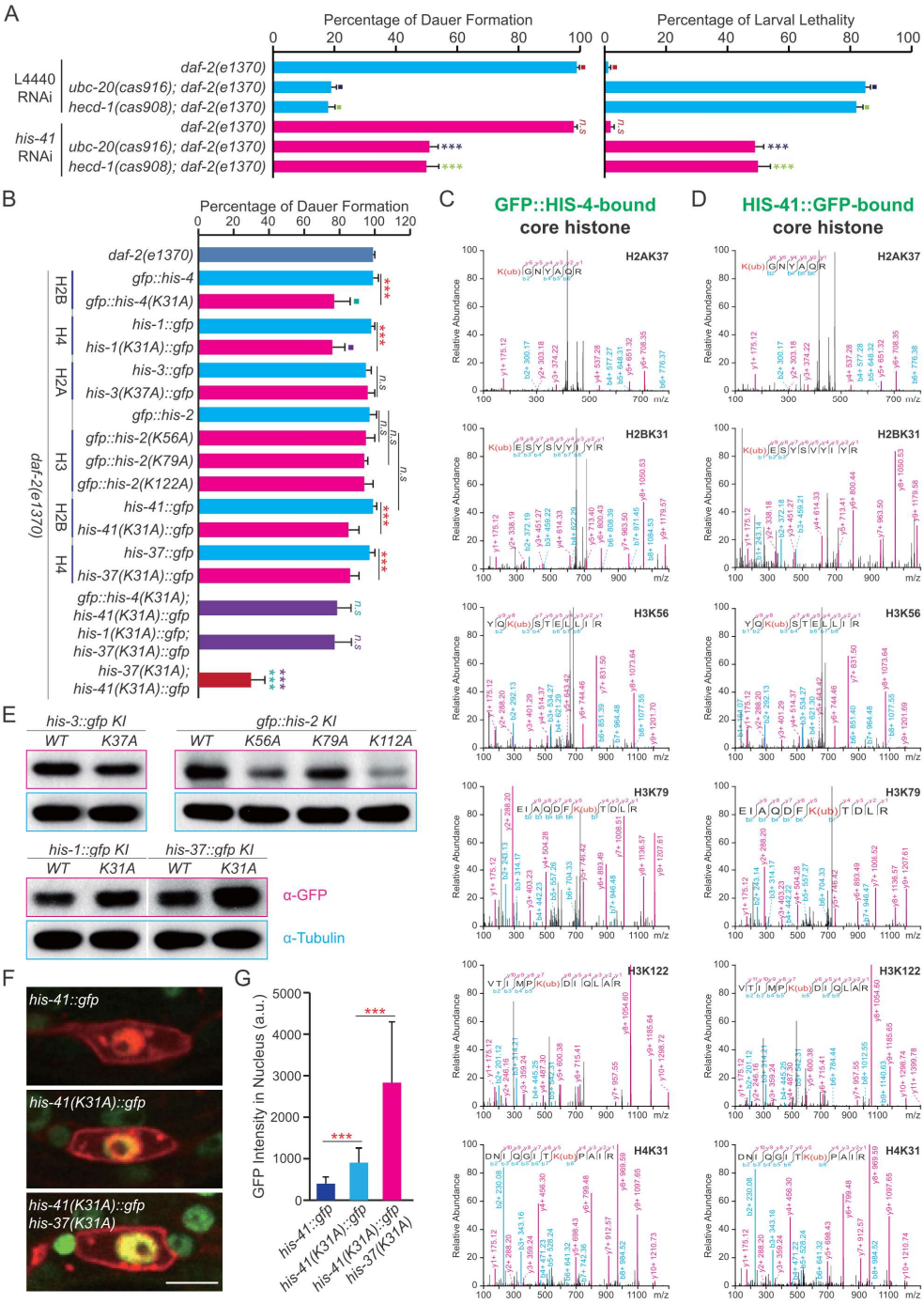

Appendix Figure S4. Histone H4K31 is required for H2B degradation. (A) Dauer formation and larval lethality in different genotypes fed with dsRNA-expressing bacteria targeting *his-41*. Six independent assays were performed, n > 100; data shown are means ± SEM; statistical significance compared with the control (■) with a

matching color; *P* values were determined by two-tailed unpaired t-test, ***$P < 0.001$, *n.s.*, no significance. **(B)** Genetic analysis of dauer formation with different genotypes. Six independent assays were performed, n > 100; data shown are means ± SEM; *P* values were determined by two-tailed unpaired t-test, ***$P < 0.001$, *n.s.*, no significance. **(C-D)** Putative ubiquitinated peptides in H2A, H2B, H3, and H4 from GFP::HIS-4 (C) or HIS-41::GFP (D) associated nucleosomes in *C. elegans*. The y and b series indicate fragments at amide bonds of the peptide. **(E)** Immunoblot of the endogenous H2A, H3, and H4 protein levels in the WT and corresponding mutants under well-fed condition. **(F)** Fluorescence images of the endogenous GFP::HIS-41(H2B) fluorescence in seam cells under well-fed condition with different genotypes. The mCherry::PH (membrane) and mCherry::HIS-24 (histone H1, nucleus) were expressed under the control of a seam cell-specific *ceh-16* promoter. Scale bar, 5 μm. **(G)** Quantification of endogenous HIS-41::GFP fluorescence in seam cells under well-fed condition with different genotypes (each genotype n = 100). Data shown are means ± SEM; *P* values were determined by two-tailed unpaired t-test, ***$P < 0.001$.

Appendix Figure S5

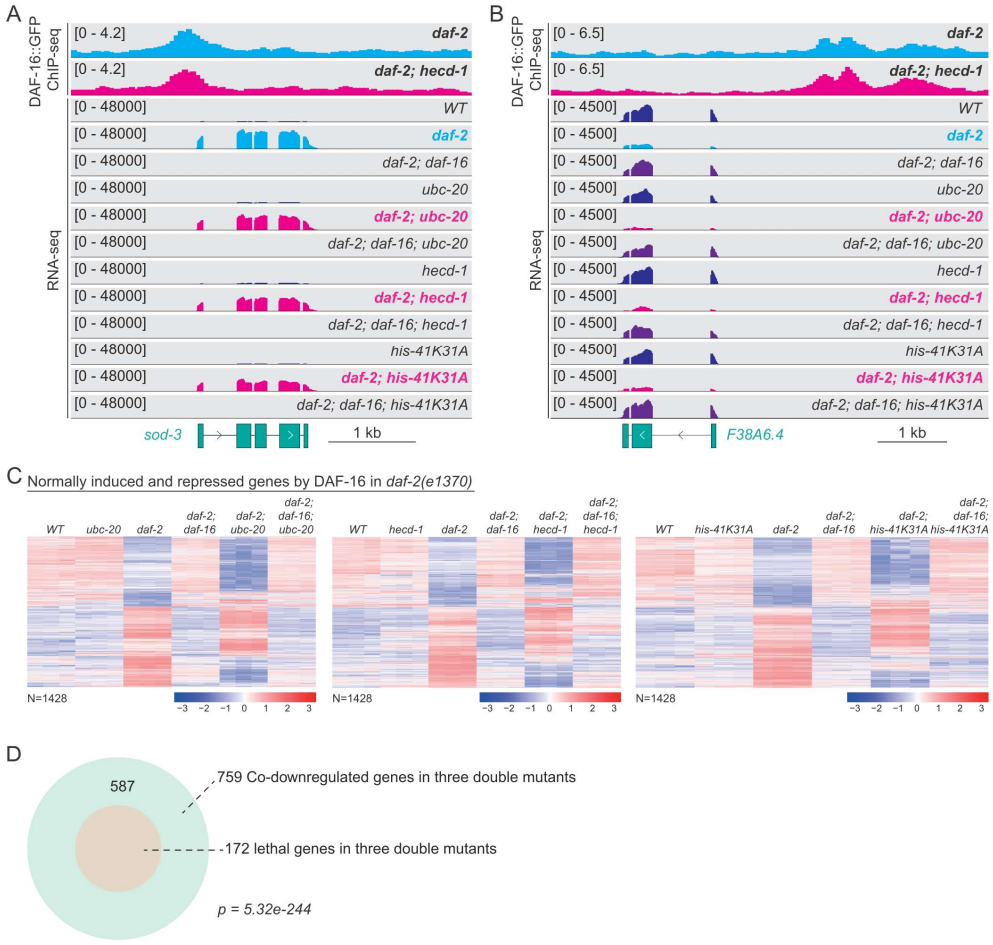

Appendix Figure S5. Inhibition of H2B degradation did not affect DAF-16-dependent gene expression for insulin/IGF-mediated Dauer formation. (A) Genome browser tracks of DAF-16::GFP ChIP-seq peaks and RNA-seq peaks with different genotypes at the *sod-3* locus. **(B)** Genome browser tracks of DAF-16::GFP ChIP-seq peaks and RNA-seq peaks with different genotypes at the *F38A6.4* locus. **(C)** Transcriptomic analysis of gene expression by DAF-16 during *daf-2*-mediated dauer formation in animals with different genotypes. Genes were induced or repressed (Fold Change > 2) in *daf-2(e1370)*, but not changed (Fold Change < 2) or reversed in *daf-2(e1370); daf-16(mu86)* mutants. **(D)** Statistical analysis of lethal genes from co-downregulated genes by DAF-16 in *daf-2; ubc-20*, *daf-2; hecd-1,* and *daf-2; his-41*^{K31A} mutants. The p value was calculated using a hypergeometric probability test.

Appendix Figure S6

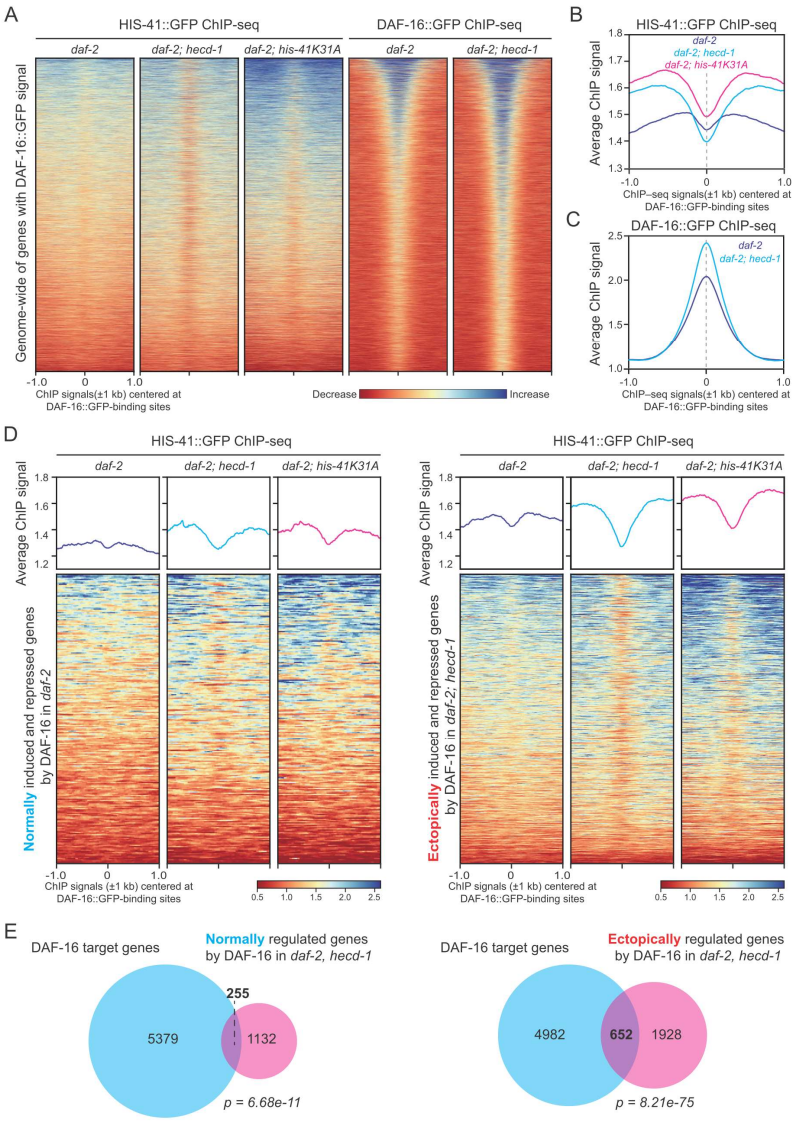

Appendix Figure S6. Inhibition of H2B degradation enhances DAF-16 binding to chromatin. (A) Heatmap view of HIS-41::GFP and DAF-16::GFP ChIP signals at DAF-16-binding sites in different genotypes. **(B)** Average of HIS-41::GFP ChIP signals at all the DAF-16-binding sites in *daf-2*, *daf-2; hecd-1,* and *daf-2; his-41*^{K31A} mutants. **(C)** Average of DAF-16::GFP ChIP signals at all the DAF-16-binding sites in *daf-2* and *daf-2; hecd-1* mutants. **(D)** Average and heatmap of HIS-41::GFP ChIP-seq signals at DAF-16-dependent normal or ectopic gene expression in *daf-2, daf-2; hecd-1,* and *daf-2; his-41*^{K31A} mutants. **(E)** Overlap analysis of genes bound by DAF-16 and genes regulated by DAF-16 in *daf-2(e1370), hecd-1(cas908)* double mutant. Genes normally

regulated by DAF-16 in the double mutant compared with *daf-2(e1370)* are shown in the left diagram; genes ectopically regulated in these comparisons are shown in the right diagram. The p value was calculated using a hypergeometric probability test.

Appendix Figure S7

A

Description	Analyzed peptide	Modifications	Charge	m/z [Da]
H2B	LLLPGELAK		2	477.31
	LLLPGELAK	13C(6)15N(2) [K9]	2	481.31
H4	DNIQGITKPAIR		3	442.58
	DNIQGITKPAIR	13C(6)15N(2) [K8]	3	445.26
H2A.z(v)	VGATAAVYSAAILEYLTAEVLELAGNASK		3	965.85
	VGATAAVYSAAILEYLTAEVLELAGNASK	13C(6)15N(2) [K29]	3	968.52
H2A	VTIAQGGVLPNIQAVLLPK		3	644.39
	VTIAQGGVLPNIQAVLLPK	13C(6)15N(2) [K19]	3	647.06
H3.1	FQSSAVMALQEACEAYLVGLFEDTNLCAIHAK	Carbamidomethyl [C13; C27]	4	897.43
	FQSSAVMALQEACEAYLVGLFEDTNLCAIHAK	Carbamidomethyl [C13; C27]; 13C(6)15N(2) [K32]	4	899.43
H3.2	FQSSAVMALQEASEAYLVGLFEDTNLCAIHAK	Carbamidomethyl [C27]	4	879.18
	FQSSAVMALQEASEAYLVGLFEDTNLCAIHAK	Carbamidomethyl [C27]; 13C(6)15N(2) [K32]	4	881.18
H3.3	FQSAAIGALQEASEAYLVGLFEDTNLCAIHAK	Carbamidomethyl [C27]	4	860.18
	FQSAAIGALQEASEAYLVGLFEDTNLCAIHAK	Carbamidomethyl [C27]; 13C(6)15N(2) [K32]	4	862.18
H1	ASGPPVSELITK		2	599.84
	ASGPPVSELITK	13C(6)15N(2) [K12]	2	603.84

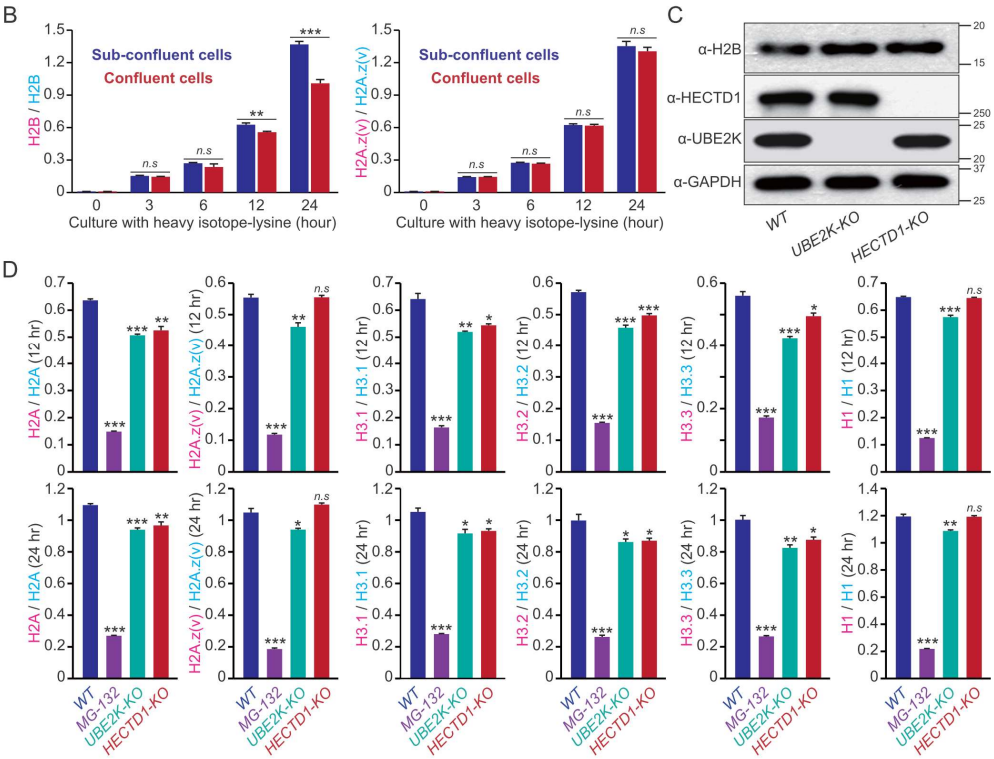

Appendix Figure S7. UPS-dependent nucleosomal histone turnover in human cells.

(A) Representative peptides of different histones from the mass spectrum used to analyze histone turnover. The old histone (K with blue color) was labeled with light amino acids, and the newly synthesized histone (K with pink color; i.e., $^{13}C_6{}^{15}N_2$ modification) was labeled with heavy amino acids. The carbamidomethyl (C) in H3 is derived from an in-gel digestion experiment. **(B)** Quantification of H2B and H2A.z(v) turnover in sub-confluent or confluent cultured WT cells. Histone H2B turnover rate is

faster in growing cells compared to quiescent cells. Notably, the histone variant H2A.v/z, which does not exhibit a cell-cycle-dependent expression pattern, shows a similar turnover rate in both sub-confluent and confluent culture cells. These results indicate that the conditions of confluent culture could minimize the effects of the cell cycle, allowing the histone turnover to reflect chromatin dynamics in a quiescence-dependent manner. Two independent assays were performed; data shown are means ± SEM; *P* values determined by two-tailed unpaired t-test, $**P < 0.01$, $***P < 0.001$. **(C)** Immunoblot of the endogenous H2B protein levels in confluent cultured *WT, UBE2K-KO,* and *HECTD1-KO* cells. **(D)** Quantification of H2A, H2A.z(v), H3.1, H3.2, H3.3, and H1 turnover in WT cells treated with DMSO or in MG-132, *UBE2K-KO,* and *HECTD1-KO* cells. Three independent assays were performed; data shown are means ± SEM; *P* values determined by two-tailed unpaired t-test, $*P < 0.05$, $**P < 0.01$, $***P < 0.001$, *n.s.*, no significance.

Appendix Figure S8

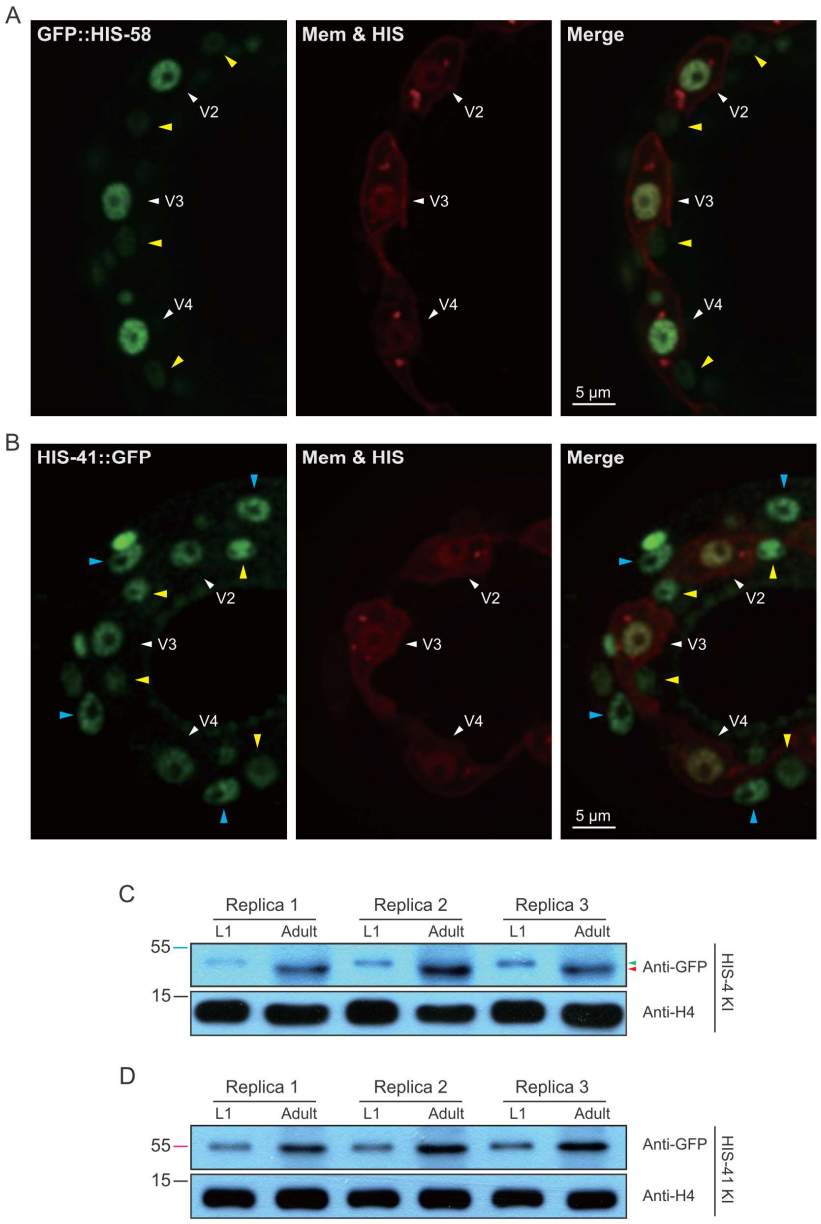

Appendix Figure S8. H2B replacement and degradation during development in *C. elegans*. (A-B) Fluorescence images of the endogenous GFP::HIS-58 KI and HIS-41::GFP KI after seam cells fused with hyp 7. The yellow arrowheads indicate the nuclei of seam cells that have just completed fusion with hyp 7. On the other hand, the blue arrowheads represent the nuclei of seam cells from a previous round of fusion with hyp 7. The mCherry::PH (membrane) and mCherry::HIS-24 (histone H1, nucleus) were expressed under the control of a seam cell-specific *ceh-16* promoter. Scale bar, 5 μm.

(C-D) Immunoblot of the endogenous GFP::HIS-4 and HIS-41::GFP in L1 and adult animals. Histone H4 was the loading control. The blue line indicated AGSGSG as the linker between GFP and H2B, and the pink line indicated TEV-S (TEV indicating TEV protease cleavage site, and S indicating S-tag) as the linker between GFP and H2B. The green arrowhead indicates GFP::HIS-4, and the red arrowhead indicates the nonspecific protein. Relative molecular weight; K, thousands.